

## Spectral Energy Distributions of Quasars and AGN

Belinda J. Wilkes

*Smithsonian Astrophysical Observatory, 60 Garden St., Cambridge MA  
02138, USA*

**Abstract.** Active Galactic Nuclei (AGN) are multiwavelength emitters. To have any hope of understanding them, or even to determine their energy output, we must observe them with many telescopes. I will review what we have learned from broad-band observations of relatively bright, low-redshift AGN over the past  $\sim 15$  years. AGN can be found at all wavelengths but each provides a different view of the intrinsic population, often with little overlap between samples selected in different wavebands. I look forward to the full view of the intrinsic population which we will obtain over the next few years with surveys using today's new, sensitive observatories. These surveys are already finding enough new and different AGN candidates to pose the question "What IS an AGN?".

### 1. Introduction

Unlike stars and galaxies, quasars and AGN are multi-wavelength emitters. As a result obtaining a complete picture of an AGN is a challenging prospect requiring observations with a wide variety of telescopes. Over the past two decades, our multi-wavelength view of quasars and AGN has expanded significantly thanks to the continuing increases in sensitivity (Sanders et al., 1989, Elvis et al. 1994, Haas et al. 1998, Polletta et al. 2000, Haas et al. 2003). The variety of the resulting Spectral Energy Distributions (SEDs) grows with our parameter space (Kuraszkiewicz et al. 2003) and, while the contributing emission and absorption mechanisms are well accepted, their relative importance, particularly as a function of AGN class, remains a subject of debate.

Also hotly debated are the importance of orientation and absorption in determining the SED, the relations between the various classes and the details of the Unification picture. While surveys at many wavelengths can efficiently find AGN, these surveys provide different views of the AGN population, always selecting those brightest in a particular waveband. It can be argued that some wavebands provide a less biased view than others, (e.g. X-rays are less affected by absorption, far-IR is independent of orientation). However it is only by combining surveys in different wavelength regions that we can gain a view of the intrinsic population. Only then can we hope to answer the many open questions that remain.

With the advent of new, sensitive observing facilities at many wavelengths (X-RAY: Chandra, XMM-Newton, IR: 2MASS, SIRTf OPTICAL: 8-m telescopes, SDSS), multi-wavelength observations are now possible for a significant

fraction of the AGN population. Deeper, multi-wavelength surveys are finding possible new varieties of AGN which raise the fundamental question: “What is an AGN?”. Examples include the numerous, low-redshift red AGN found by 2MASS (Cutri et al., 2001) and otherwise uninteresting, X-ray loud galaxies visible with Chandra (Brandt et al. 2001). Whether these new sources are truly AGN, how they relate to “traditional” AGN and how large a fraction of the population they constitute, are major open questions which will be addressed via multi-wavelength follow-up.

Although AGN can be found in many wavebands, definitive classification is challenging without optical/IR spectroscopic data. This is particularly true given the lack of correspondence between the traditional optical class and other characteristics in increasing subsets of the population (e.g. IR/optical emission lines and X-ray flux (Genzel & Cesarsky 2000), or optical class and X-ray absorption (Wilkes et al. 2002)). The SDSS is providing an unprecedentedly large sample to relatively faint optical flux limits, the means to classify AGN with a wide range of SEDs. Similarly, SIRTf, successfully launched in August 2003, will fill the last major gap in our multi-wavelength picture of AGN reaching beyond the few bright and/or nearby sources, to the bulk of the population in the mid- and far-IR for the first time.

With this unprecedented combination of powerful, multi-wavelength observatories and the many planned and in progress surveys being carried out (GOODS: Giavalisco et al. 2003, ChaMP: Kim et al, 2003a, SWIRE: Lonsdale et al, 2003), we are poised to take great strides in our understanding of the intrinsic population of AGN, and their structure and evolution, as well as the larger question of the importance of accretion to the energy budget of the universe.

In this article, I review the observational components of AGN SEDs along with the physical structure and emission mechanisms believed to contribute in the various wavebands. The shape and variety of the SEDs, colors, flux ratios and other properties are discussed as a function of AGN properties and in comparison with models. I conclude with the prospects for answering the question: “What is an AGN?” and thus of viewing the intrinsic population and constraining AGN models.

## 2. The AGN Spectral Energy Distribution Observed

### 2.1. General Characteristics

Figure 1 shows examples of fairly well-observed SEDs for both a radio-quiet (RQQ) and a radio-loud (RLQ) quasar. Both classes show peaks in their energy output in the infra-red (IR bump) and optical (“Big Blue Bump”) wavebands. The IR bump is generally attributed to thermal emission from dust at a wide range of temperatures,  $\sim 50\text{--}1000$  K and the Big Blue Bump in thermal emission from the gas in an accretion disk. The relative strengths of the IR and Big Blue bumps varies but they are generally comparable. The inflection between the two peaks, at  $\sim 1.5\mu\text{ m}$ , is due to the maximum dust temperature of  $\sim 2000\text{K}$  caused by sublimation (Sanders et al. 1989). In the X-ray region,  $\sim 50\%$  of both RLQs and RQQs have a soft X-ray excess component thought to be the high energy tail of the Big Blue Bump.

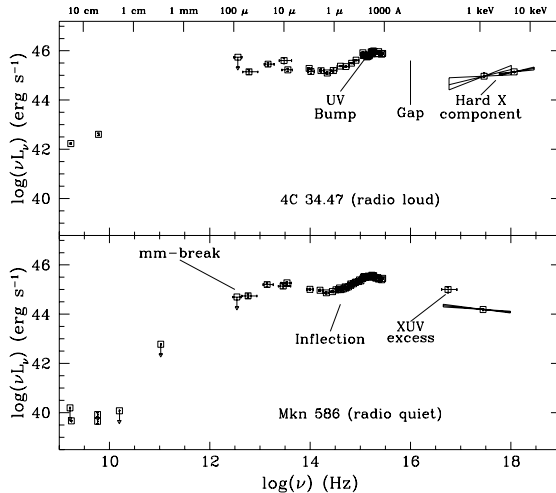


Figure 1. Radio – X-ray spectral energy distribution of radio-loud (upper) and radio-quiet (lower) quasar, Elvis et al. (1994).

At harder X-ray energies, power law emission has differing slopes and relative strengths. RQQs typically have slope,  $\alpha_E \sim 1.0 \pm 0.5$  (where  $F_\nu \propto \nu^{-\alpha_E}$ , the range indicates a real spread in the observed slopes), while in RLQs the slope is flatter ( $\sim 0.5 \pm 0.5$ ) and the relative normalisation about  $\times 3$  higher (Wilkes & Elvis 1987, Reeves & Turner 2000). The emission mechanisms are different: comptonisation of EUV photons in the Big Blue Bump for RQQs (Gondek et al. 1996) and synchrotron self-Compton scattering of the radio photons in RLQs. In lower luminosity AGN reflected and/or scattered emission from cold/hot material surrounding the X-ray source, such as a corona around the AD or the inner edge of the dusty torus/disk (Mushotzky et al. 1993, Turner et al. 1997, Nandra et al. 1997, Pounds et al. 2001), often dominate the underlying power law. Strong Fe  $K\alpha$  emission, originating in cold and/or hot material, is present in many low luminosity AGN but weaker/absent at higher luminosities (Reeves & Turner 2000). Please see Brandt (this volume) for a more detailed review of the X-ray emission of AGN.

The most notable difference between RLQs and RQQs is in the radio waveband. In RQQs the SED turns over sharply in the far-IR/mm and radio emission is  $\sim 100 - 1000\times$  weaker than in RLQs. In RLQs the IR–radio continuum is smooth with non-thermal emission contributing in both wavebands (Figure 2).

The far-IR cut-off in RQQs is well-determined in only a small number of nearby sources which are bright in the far-IR. Constraints on its slope are frequently steeper than the  $\nu^{2.5}$  characteristic of homogeneous synchrotron self-absorption. Instead the far-IR emission is identified as grey-body emission from cool dust (Chini et al. 1989, Hughes et al. 1993)

By contrast, the far-IR emission from core-dominated RLQs smoothly extends into the radio, implying a significant/dominant non-thermal component in both wavebands (Figure 2). 3C273 exhibits the correlated variability characteristic of blazars (core-dominated RLQs viewed pole-on), but even here the lack of variability in the hottest part of the IR continuum indicates the presence of hot dust (Tuerler et al. 1999). ESA’s Infrared Space Observatory (ISO), the

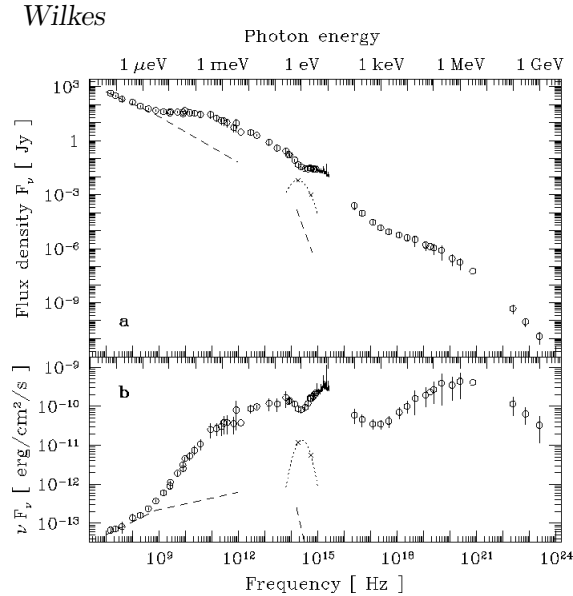


Figure 2. The radio– $\gamma$ -ray SED of 3C273 on (a)  $F_\nu$  and (b)  $\nu F_\nu$  scale (Tuerler et al. 1999) showing the smooth, radio–IR continuum emission typical of core-dominated RLQs.

most sensitive IR satellite to date (prior to SIRTf, launched earlier this year), facilitated observation of a larger number of quasars and AGN than in the past. Comparison of the IR continua of RLQs and RQQs suggests that non-thermal IR emission dominates pole-on RLQs but decreases in strength as the viewing angle increases so that thermal emission also contributes in lobe-dominated RLQs (Haas et al. 1998, Polletta et al. 2000).

While both sources in Figure 1 are typical of the SEDs of broad-lined quasars in their class, the relative strengths of the various components range by  $\sim$  an order-of-magnitude from source to source, even within the X-ray-bright subset of the population (Elvis et al. 1994). This variety increases with less biased selection techniques such as the X-ray (Kurasziewicz et al. 2003).

In the past 9 years since Figure 1 was published many more SEDs, mainly of low-redshift AGN, have been observed. SEDs have many more data points, particularly in the IR and submm region where ISO, IRAM and the JCMT have made significant steps forward. However the general picture of the SEDs of “normal” AGN has not changed significantly. What has changed much more is our concept of what IS an AGN.

## 2.2. Origin of the various components

The physical picture for the origin of these components is based on Unification of the AGN classes (Miller & Antonucci 1983, Barthel 1989). The quasar’s central super-massive ( $10^{7-9} M_\odot$ ) black hole is surrounded by hot accreting gas, primarily confined to an accretion disk (AD), emitting optical and UV radiation to provide the Big Blue Bump. The IR bump originates in dust with a wide range of temperatures, the hottest being directly associated with the AGN

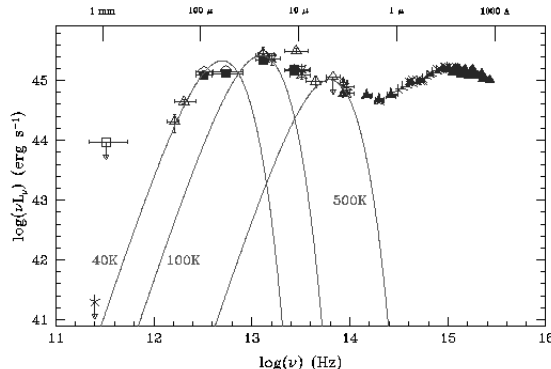


Figure 3. mm–optical spectral energy distribution of PG1351+640 showing the wide range of temperature required to explain the full IR emission as thermal emission from dust. The curves show grey bodies at the marked temperatures normalised to “fit” the data.

while the cooler dust originates in the host galaxy, again with a disk-like/torus geometry. X-ray and radio emission from the core varies on short timescales ( $\sim 1 - 100$  lt. days) and so originates close to the central black hole, interior to the AD. Some AGN ( $\sim 10\%$ ) have extended radio structure from jets and lobes on much larger scales which will not be discussed here.

In a simple unification scenario broad-lined (Type 1) AGN are viewed face-on while in narrow-lined (Type 2) AGN the broad emission line region (BELR) the soft X-rays and much of the optical/UV emission from the AD are hidden by the dust. The SEDs of type 2 AGN have less prominent Big Blue Bumps and strong soft X-ray absorption than their type 1 counterparts. Comparisons between type 1 and 2 AGN at low redshift (Seyfert 1 and 2), where most known Sy2s reside, agree with these expectations. Their relatively low luminosities result in their optical continua including a significant contribution from the host galaxy within which the central black hole and AGN reside.

To explain the broad IR continuum (Figure 3) using pure thermal emission, the dust must have a wide range of temperatures ( $\sim 50 - 1000$ K). Based upon the presence of extended dust emission in nearby AGN (e.g. Cen A, Genzel & Cesarsky 2000), strong correlations between hot mid-IR emission and the presence of an AGN (Heisler & de Robertis 1999) and weaker correlations between far-IR emission and other AGN indicators (Andreani et al. 2003), the IR continuum has been modeled using 2/3 components. A hot, obscuring dusty torus in an AGN (Pier & Krolik 1992, Granato & Danese 1994) produces a narrow continuum feature which is combined with a cooler, starburst component (Efstathiou & Rowan-Robinson 1995, Rowan-Robinson 2000). Cool dust in the host galaxy may also contribute.

### 3. How well does the picture fit?

#### 3.1. The Optical/UV Big Blue Bump

The Big Blue Bump can be explained as thermal emission from gas in an accretion disk (AD) with a wide range of temperatures. ADs have a large number of

parameters and can produce the variety of observed SED shapes (Siemiginowska et al. 1995). Individual fits which include the soft X-ray excess require scattering of the AD photons in a lower density, hot corona (Zycki et al. 1995, Laor et al. 1997). As noted by Blaes (this volume), to further constrain accretion disk models, an observational relation between optical/UV colors and the black hole mass are required. Mass measurements are available for a small number of low-redshift sources, although new methods have been developed to estimate the mass at higher redshift (Vestergaard, this volume).

As popular as accretion disks are, they are not unique in being able to explain the optical–soft X-ray continuum of AGN. Models invoking mildly optically thick cloud distributions (Czerny & Dumont 1998, Collin-Souffrin et al. 1996) provide an alternative.

### 3.2. IR continuum

Spectroscopic observations from ISO (Clavel et al. 1998) show a stronger near-mid IR continuum in Sy1 than in Sy2 galaxies causing a lower observed equivalent width  $7.7 \mu\text{m}$  feature in Sy1s. Orientation dependent near-IR emission is also clear from comparison of Sy2s with and without hidden broad line regions (Heisler et al. 1997). Further comparison with Sy1s and quasars (Figure 4, Kuraszkiwicz et al. 2003) indicate obscuring column densities,  $\log N_{\text{H}} \sim 23$ , as opposed to  $\sim 24$  in earlier torus models (Pier & Krolik 1992). Lower column density (Kuraszkiwicz et al. 2003) or clumpy (Zier & Biermann 2002, Nenkova et al. 2002) models for the obscuring material reproduce the full range of temperatures in AGN IR continua with orientation primarily responsible for the range in IR SED shapes. This removes the need for a starburst-related component (Kuraszkiwicz et al. 2003), although a two-component model is required in some low-redshift AGN (Genzel & Cesarsky 2000).

An alternative suggestion invokes evolution to explain at least part of the range IR continuum shapes (Haas et al. 2003). In this scenario (Sanders et al. 1988) IR galaxies are young quasars/AGN where the central engine is obscured by dust. The SED then changes from a young state where the far-IR continuum dominates, through an AGN state in which the IR continuum is hotter and the Big Blue Bump appears and on to a dead quasar where the latter component disappears. Although such a model can, qualitatively, explain the range of SEDs observed in the PG sample (Haas et al. 2003), there is no definitive evidence connecting SED shape to the evolution/age of a source.

### 3.3. Orientation, obscuration and AGN Class

The unification scenario that type 2 AGNs are viewed through optically thick material which hides the BELR and the central continuum source is supported statistically by the general tendency for type 2 AGN to have absorbed X-ray spectra (Turner et al. 1997, Awaki et al. 1997), a redder optical continuum, and stronger galactic spectral features. Individual sources are less straight-forward. Optical dust reddening is generally lower than the equivalent X-ray gas absorption (Maiolino et al. 2001, Risaliti et al. 2001). A few sources have been seen to change type, with broad emission lines appearing/disappearing and/or X-ray absorption varying (Matt et al. 2003). Some type 1 or intermediate sources have strong X-ray absorption (Page et al. 2001) and there is little relation between

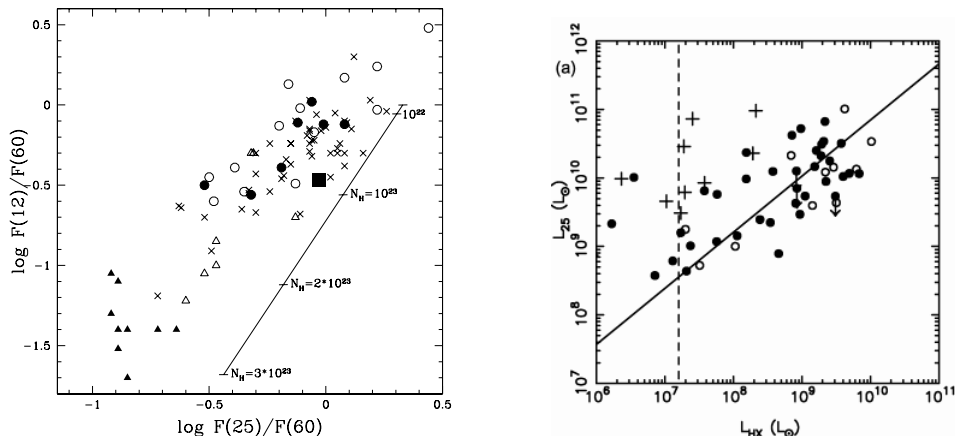


Figure 4. Left: Mid-IR colors for quasars compared with Seyfert 2 galaxies (Heisler et al. 1997) showing that reddening of up to  $\log N_H \sim 23$  can explain the progression (Kuraskiewicz et al. 2003, Fig.11). Right: The effects of host galaxy emission on the mid-IR colors of low luminosity AGN (Lumsden & Alexander 2001).

X-ray hardness ratio and AGN class (Wilkes et al. 2002, Figure 5). These results imply a more complex obscuring medium than the optically thick torus originally suggested. Current scenarios generally involve high velocity, accelerating winds originating in a disk (Konigl & Kartje 1994, Murray & Chiang 1995, Konigl this volume, Elvis this volume). These models can also explain the high excitation, broad-absorption lines visible in  $\sim 10\%$  of type 1 AGN. Variations and differing lines-of-sight to continuum and line regions due to clumpiness and variation in the wind itself can explain the variety of properties seen in individual sources. However to provide real constraints on the structure and geometry of the absorbing material, we need multi-wavelength observations of the intermediate sources discussed above.

### 3.4. The Effects of Luminosity

Sy2s, which are lower luminosity and more obscured than Sy1s, often show optical/UV host galaxy spectral features. Galaxy light peaks in the wavelength region close to the minimum between the IR and OUV bumps in AGN so the strength of this inflection depends on the relative luminosity of the AGN and its host. Thus the near-IR is the best region in which to study the host galaxy (McLeod & Reike 1995). Host galaxy emission may also contribute to the near- and mid-IR continuum (Figure 4, Lumsden & Alexander 2001) and the optical continuum (Maiolino et al. 2000).

### 3.5. Ingredients which determine the Shape of the SED

Many parameters are important in determining the observed shape of an AGN SED. The relative luminosities of the AGN itself, related to the black hole mass, and of its host galaxy determine the visibility of host galaxy emission. The accretion rate and physical properties of the AD combine with its inclination to

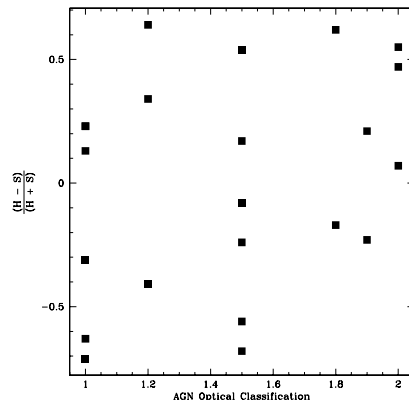


Figure 5. X-ray hardness ratios determined by the *Chandra* for 2MASS red AGN (Wilkes et al. 2002), as a function of optical class demonstrating the lack of a relation between the two in this sample.

our line-of-sight to determine the shape of the Big Blue Bump. The amount, geometry, ionisation and optical depth of absorbing dust and gas and its inclination determines the IR continuum and the absorption of the optical, near-IR and soft X-ray continua. The amount and location of scattering material and the strength of the scattered light is also important in edge-on (type 2) AGN where the primary AGN continuum is partially/fully obscured. Finally the presence and strength of a radio source in the core of the AGN affects the radio, far-IR and hard X-ray continua.

One property which, perhaps surprisingly, has not yet been shown to be related to the SED is evolution. With the central black hole as driver of the energy source, the black hole is expected to grow as material is accreted and so the observable properties of the AGN are expected to change as the source ages. Although observations of high redshift AGN/quasars are still limited, there is currently no convincing evidence for a change in SED with redshift (Silverman et al. 2002, Mathur et al. 2002, Brandt et al. 2002, Vignali et al. 2003). Similarly, as discussed earlier, evolution may unify ULIRGs and AGN predicting changes in the IR SED as the dust first enshrouds and then heats up and disperses, allowing the AGN to shine through. While the OUV and IR SEDs show a wide diversity of shapes, there is no compelling evidence for systematic evolution in their properties as a function of redshift. The much larger number of high-redshift AGN now accessible in many wavebands will provide significant new data on SED evolution.

#### 4. Our Expanding View of AGN

With so many variables, it is not surprising that AGN SEDs are so diverse, it may be more surprising that we see such similarities from source to source! This leads to the question of selection. Are they mostly similar because we select them to be? Would we recognise an AGN that was, for example, so heavily absorbed that few if any of the general characteristics we associate with an AGN are present? Motivated by the large number of apparently normal galaxies being



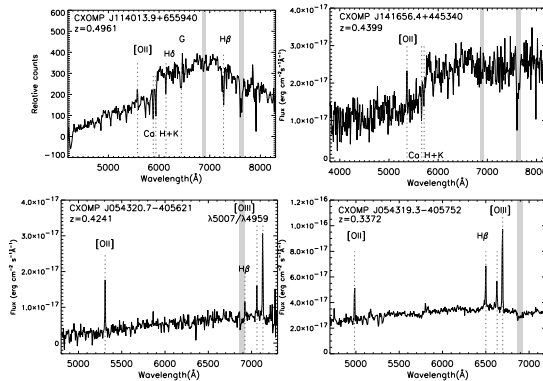


Figure 6. Candidate buried AGN, ChaMP survey, Green et al. (2004).

found by the Chandra Deep Surveys, Moran et al. (2002) show how host galaxy light may dominate optical AGN signatures in Sy2s and thus hide a significant fraction of the population.

Thus, perhaps the most critical open question is “What is an AGN?”. New AGN are being found in radio (Webster et al., 1995), IR (Cutri et al. 2001) and deeper optical surveys, 2DF and SDSS (Richards et al. 2003). Models for the Cosmic X-ray Background (CXRB) require a new population of X-ray absorbed AGN (Gilli et al. 2001). Chandra and XMM-Newton find X-ray sources sufficiently luminous to be AGN but with no optical AGN characteristics (Figure 6, Green et al. 2004 (ChaMP), Norman et al. 2002). Similarly, bright radio galaxies with strong, unresolved cores show no optical AGN signatures. Are these all AGN? If so how do we relate them to the more standard BEL AGN? What are a minimum set of properties which define an AGN? How can we observe the intrinsic population?

Since AGN are multiwavelength emitters, we need a view in multiple wavebands. For example the red AGN found in the 2MASS survey are hard, weak X-ray sources (Wilkes et al. 2002) and may contribute  $\sim 30\%$  of the CXRB depending on their evolution (Figure 7, Wilkes et al. 2003). But X-ray surveys must cover more area to deeper flux levels to find the same kinds of sources. The next generation of multi-wavelength surveys will provide both deep, small areas (GOODS) and shallower, wider areas (SWIRE; ChaMP, Silverman, this volume) and sample the same/overlapping pieces of the intrinsic population. The combination of sensitive IR and X-ray, provided by *Chandra*, XMM-Newton and SIRTf, is particularly powerful as the far-IR sees all luminous IR sources while the X-rays select the AGN from amongst the predominant IR galaxy population. These are exciting times!

## References

- Andreani, P. et al., 2003, AJ, 125, 444  
 Awaki, H. et al., 1997, AdSpR, 19, 95  
 Barthel, P.D., 1989, ApJ, 336, 606

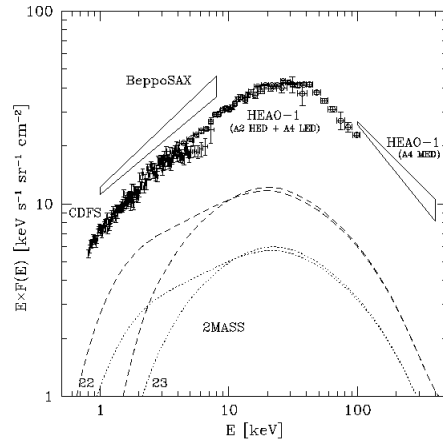


Figure 7. Contribution of 2MASS red AGN to the CXRB for two different evolutionary models, Wilkes et al. 2003

- Brandt, W. N., et al., 2001, *AJ*, 122, 2810  
 Brandt, W.N., et al., 2002, *ApJ*, 569, 5  
 Chini, R., Kreysa, E. & Biermann, P.L., 1989, *AA*, 219, 87  
 Clavel, J. et al., 2000, *AA*, 357, 839  
 Collin-Souffrin, S., Czerny, B., Dumont, A.-M., Zycki, P. T., 1996, *AA*, 314, 393  
 Cutri, R.M. et al., 2001, *ASP Conf.Ser.*, 232, 78  
 Czerny, B. & Dumont, A-M., 1998, *AA*, 338, 386  
 Efstathiou, A. & Rowan-Robinson, M., 1995, *MNRAS*, 273, 649  
 Elvis, M., Wilkes, B.J., et al., 1994 *ApJ*, 95, 1  
 Genzel, R. & Cesarsky, C.J., 2000, *ARAA*, 38, 761  
 Giavalisco, M. et al., 2003, *ApJL in press* (astro-ph/0309105)  
 Gilli, R., Salvati, M. & Hasinger, G., 2001, *AA*, 366, 407  
 Green, P.J., et al., 2004, *ApJS*, 150 *in press* (astro-ph0308506)  
 Gondek, D. et al., 1996, *MNRAS*, 282, 646  
 Granato, G.L. & Danese, D.L., 1994, 268, 235  
 Haas, M. et al., 2003, *AA*, 402, 87  
 Haas, M. et al., 1998, *ApJ*, 503, L109  
 Heisler, C.A. & de Robertis, M.M., 1999, *AJ*, 118, 2038  
 Heisler, C. A., Lumsden, S. L., & Bailey, J. A. 1997, *Nature*, 385, 700  
 Hughes, D.H. et al., 1993, *MNRAS*, 263, 607  
 Kim, D-W., 2004a, *ApJ*, 600, *in press* (astro-ph/0308493)  
 Kim, D-W., 2004b, *ApJS*, 150, *in press* (astro-ph/0308492)  
 Konigl, A. & Kartje, J.F., 1994, *ApJ*, 434, 446  
 Kuraszewicz, J.K. et al., 2003, *ApJ*, 590, 128  
 Laor, A., Fiore, F., Elvis, M., Wilkes, B. & McDowell, J., 1997, *ApJ*, 477, 93  
 Lonsdale, C.J., et al., 2003, *PASP*, 115, 897

- Lumsden, S.L. & Alexander, D.M., 2001, MNRAS, 328, 32
- Maiolino, R. et al. 2000, AA, 355, 47
- Maiolino, R. et al., 2001, AA, 365, 28
- Mathur, S., Wilkes, B.J., Ghosh, H., 2002, ApJ, 570, 5
- Matt, G., Guainazzi, M. & Maiolino, R., 2003, MNRAS, 342, 422
- McLeod, K.K. & Rieke, G.H., 1995, ApJ, 441, 96
- Miller, J.S. & Antonucci, R.R.J., 1983, ApJ, 271, 7
- Moran, E.C., Filippenki, A.V. & Chornock, R. 2002, ApJ, 579, 71
- Murray, N., Chiang, J., Grossman, S.A & Voit, G.M., 1995, ApJ, 451, 498
- Mushotzky, R.F., Done, C., & Pounds, K.A., 1993, ARAA, 31, 717
- Nandra, K. et al., 1997 ApJ, 477, 602
- Nenkova, M., Ivezić, Z. & Elitzur, M., 2002, ApJ, 570, 9
- Norman, C. et al, 2002, ApJ, 571, 218
- Page, M., Mittaz, J.P.D. & Carrera, F.J., 2001, MNRAS, 325, 575
- Pier, E.A., & Krolik, J.H. 1992, ApJ, 401, 99
- Polletta, M., Courvoisier, T., Hooper, E., Wilkes, B., 2000, AA, 362, 75
- Pounds, K.A., et al., 2001, ApJ, 559, 181
- Reeves, J.N. & Turner, M.J.L., 2000, MNRAS, 316, 243
- Richards, G.T. et al., 2003, AJ, 126, 1131
- Risaliti, G. et al., 2001, AA, 371, 37
- Rowan-Robinson, M., 2000, MNRAS, 316, 885
- Sanders, D.B. et al., 1989, ApJ, 347, 29
- Sanders, D. B. et al., 1988, ApJ 325, 74
- Siemiginowska, A. et al., 1995, ApJ, 454, 77
- Silverman J.D. et al., 2002, ApJ, 569, 1
- Tuerler, M., Paltani, S., Courvoisier, T.J-L., et al., 1999, AAS, 134, 89
- Turner, T.J., George, I.M., Nandra, K., Mushotzky, R., 1997, ApJ, 488, 164
- Vignali, C., Brandt, W.N., Schneider, D. P., 2003, AJ, 125, 418
- Webster, R.L. et al., 1995, Nat, 375, 469
- Wilkes, B.J. et al. 2002, ApJL, 564, 65
- Wilkes, B.J., Risaliti, G. et al., 2003, *in preparation*
- Wilkes, B.J. & Elvis, M.S., 1987, ApJ, 323, 243
- Zdziarski, A. et al., 2003, MNRAS, 342, 355
- Zier, C. & Biermann, P.L., 2002, ApJ, 396, 91
- Zycki, P.T., Collin-Souffrin, S. & Czerny, B., 1995, MNRAS, 277, 70